Diagnostic Ultrasound Tooth Imaging using Fractional Fourier Transform

Sevan Harput, Tony Evans[†], Nigel Bubb[‡], and Steven Freear, *Member, IEEE*
Ultrasound Group, School of Electronic and Electrical Engineering, University of Leeds.
[†]Division of Medical Physics, University of Leeds. [‡]Oral Biology, University of Leeds.

***Abstract*—An ultrasound contact imaging method is proposed to measure the enamel thickness in human tooth. A delay-line transducer with a working frequency of 15 MHz is chosen to achieve a minimum resolvable distance of 400 μm in human enamel. To confirm the contact between the tooth and the transducer, a verification technique based on the phase shift upon reflection is used. Because of the high attenuation in human teeth, linear frequency modulated chirp excitation and pulse compression are exploited to increase the penetration depth and improve the signal-to-noise ratio. Preliminary measurements show that the enamel-dentin boundary creates numerous internal reflections, which cause the applied chirp signals to interfere arbitrarily. In this work, the fractional Fourier transform (FrFT) is employed for the first time in dental imaging to separate chirp signals overlapping in both time and frequency domains. The overlapped chirps are compressed using the FrFT and matched filter techniques. Micro-CT is used for validation of the ultrasound measurements for both techniques. For a human molar, thickness of the enamel layer is measured with an average error of 5.5% after compressing with the FrFT and 13.4% after compressing with the matched filter based on average speed of sound in human teeth.**

***Index Terms*—Echodentography, tooth imaging, fractional Fourier transform, coded excitation, linear frequency modulation.**

I. Introduction

THE first ultrasonic observations in dental tissue started in the 1960s using the pulse-echo technique to evaluate the tooth enamel, dentino-enamel junction (DEJ) and dentin-pulp interface [1], [2]. Most of these studies used simple time of flight measurements by calculating time delay between the peaks of consecutive reflections utilizing little or no signal processing techniques [1], [2], [3]. Traditionally, short-duration pulses are preferred by researchers to achieve better axial resolution. Some signal and image processing techniques, such as filtering and envelope detection, were subsequently used to improve image quality [4], [5]. However, the usage of coded excitation techniques in echodentography (ultrasound dental imaging) is not reported. In this work, a linear frequency modulated (LFM) chirp is chosen as an excitation technique to improve the signal-to-noise ratio (SNR), penetration depth and thus the image quality.

The first studies in echodentography started with the frequency range of 6-18 MHz with basic pulse-echo measurements [1], [2]. Later, some researchers are focused on high frequency ultrasound to achieve a better resolution. Hughes *et al.* have reported the use of a 35 MHz focused ultrasound piezocomposite transducer for tooth measurements [6]. Scanning acoustic microscopy (SAM) has been successfully used to image the elastic properties of carious human teeth, characterize the enamel and detect the enamel-dentin interface [7], [8], [9]. SAM has been described at frequencies around 50 MHz [7], but the highest frequency ever reported was 900 MHz by Raum *et al.* for tooth characterization [9]. SAM can be easily achieve sub-millimeter resolution, however it is not a practical diagnostic method for dentistry. Recently, the frequency range of 10-20 MHz is more commonly preferred by researchers due to the high attenuation in human tooth at higher frequencies [10], [3], [11], [12]. For this reason, a delay-line transducer with a 15 MHz center frequency is chosen in this study for the experiments. An extended and well detailed literature review of all diagnostic applications of ultrasound in dentistry has been published by Ghorayeb *et al.* [13].

The aim of this work is to measure the thickness of the enamel layer, locate discontinuities and produce an image of the tooth *ex-vivo* using ultrasound, which may provide a significant benefit to patients and dentists. In addition, *a priori* knowledge of tooth anatomy allows the early identification of cracks, decays, enamel loss or other tooth defects, which can cause inflammation or infection. According to American Association of Endodontics, it is estimated that 15 million teeth receive endodontic treatment each year in the USA [14]; early diagnostic information may help dentists reduce this number. By considering the significance of early detection of these anomalies on prevention, this work will focus on dental erosion. Dental erosion or acid erosion is mostly related with the consumption of carbonated drinks and it can cause irreversible tooth loss. It is one of the most common chronic diseases in children with 32% of 14 years showing erosion of permanent dentition [15]. The rise in consumption of sugar, coffee, and acidic beverages and disorders, such as Gastroesophageal Reflux Disease, causes dental erosion and enamel loss [4]. Monitoring the enamel thickness can provide dentists with sufficient information to prevent the enamel loss [16].

In this study, LFM excitation is used to achieve better penetration without degradation of the resolution and the fractional Fourier transform (FrFT) is utilized to analyze overlapping echoes, which is caused by the successive reflections inside the enamel and dentin layers. A tooth phantom is constructed to test the effectiveness of the proposed technique and the exper-

Sevan Harput and Steven Freear are with the Ultrasound Group, School of Electronic and Electrical Engineering, University of Leeds, Leeds, LS2 9JT, UK. E-mail: s.harput@leeds.ac.uk, s.freear@leeds.ac.uk

TABLE I
ACOUSTIC PROPERTIES OF MATERIALS

MATERIAL	Velocity (m/s)	Density (kg/m^3)	Impedance (MRayl)
Enamel[a]	6250	3000	18.8
Dentin[a]	3800	2000	7.6
Pulp[a]	1570	1000	1.57
Glass, borosilicate*	6025	2475	14.9
Dental Composite*	3350	2200	7.4
Water[b]	1482	1000	1.5
Glycerin*	1910	1265	2.42
Delay-line, polystyrene*	2310	1070	2.47
Transducer, PZT-5A[b]	4350	7750	33.7

[a] values are taken from [13]. [b] values are taken from [17].

* values are determined in our laboratory.

imental measurements are performed in the tooth phantom and an extracted human molar. To perform pulse compression on overlapping chirps, the FrFT and matched filter techniques are applied. Micro-CT, again a non-destructive imaging method, is used for validation of the proposed technique.

II. SIGNAL PROCESSING

Two of the greatest problems encountered by researchers who have applied medical ultrasound imaging techniques to dentistry are the dimensions of teeth and the varying speed of sound in the different tooth layers. In addition, the speed of sound in enamel and dentin layers is much higher than in any soft tissue [2]. These two facts inevitably suggest the use of high frequency excitation and short pulse duration for better resolution. However, the ultrasonic attenuation in dental tissue makes signal detection more difficult for high frequency pulses. The excitation pressure may be increased to achieve better penetration depth, but this is at the cost of increased intensity levels and the likely generation of harmonic signals. Long duration excitation provides a better penetration and improved SNR by increasing the excitation energy without changing the peak pressure level, but introduces another problem when the duration of the ultrasound signal is longer than the time of the round trip in that tooth layer. The signal overlapping caused by the successive reflections inside the enamel and dentin layers makes time and frequency analysis nearly impossible since both constructive and destructive interference occurs between individual reflections. Due to these reverberations, the received echoes are not identifiable in the time domain. In the frequency domain all reflections completely overlap with each other, where they are not in phase with the successive reflections. Without filtering, the resulting waveform cannot be used to determine the tooth layers.

The proposed solution in this work is to use LFM chirp excitation by exploiting the fractional Fourier technique. The FrFT allows frequency modulated signals overlapping in time and frequency to be separated.

A. Coded Excitation

Coded excitation has been shown to be effective in radar applications [18] as well as some medical ultrasound systems [19] by improving the SNR, penetration depth or image quality. Different methods such as frequency modulation, phase modulation and Golay codes are compared to find the most suitable coded excitation technique for ultrasound dental imaging. Linear frequency modulated chirp signal is chosen as an excitation technique, since it is reported to have lower side-lobe levels after compression under high attenuation and nonlinearity [20].

The complex representation of a linear frequency modulated signal is

$$s(t) = A(t) \cdot e^{j2\pi\phi(t)}, \quad 0 \le t \le T \tag{1}$$

for

$$\phi(t) = \left(f_c - \frac{B}{2}\right) t + \frac{B}{2T} t^2, \tag{2}$$

where $A(t)$ is the envelope of the signal, f_c is the centre frequency, T is the duration, and B is the bandwidth, where $f_c - B/2$ explicitly denotes the starting frequency of the chirp.

B. Matched Filter

The matched filter (MF) is the most common method for filtering and compressing chirp signals, where it optimizes the probability of detection and maximizes the SNR [19]. Therefore, MF is chosen for comparison with FrFT. Using the likelihood criterion, it can be said that the ideal filter at the receiver side must be same with the transmitted signal. Therefore, matched filter is an ideal linear time invariant filter, which maximizes the SNR [19].

In order to design an optimal receiver, the matched filter's impulse response, $h(t)$, must be equal to the complex conjugate of time reversal of the transmitted signal. It can also have a gain of k and time shift, τ_d, for physical realization. For the complex signal $s(t)$, the impulse response of the matched filter is given by:

$$h(t) = k \cdot s^*(\tau_d - t) \tag{3}$$

C. Fractional Fourier Transform (FrFT)

The fractional Fourier transform was first introduced by Namias [21] in its incomplete form. An extended analysis of FrFT was published by McBride and Kerr [22] upon which most more recent work is based. The FrFT can be expressed as

$$X_\alpha(t_\alpha) = \int_{-\infty}^{\infty} x(t)\, K_\alpha(t_\alpha, t)\, dt \tag{4}$$

where α defines the order of the transform, $K_\alpha(t_\alpha, t)$ is the transform kernel and t_α denotes the variable in the α-th order fractional Fourier domain, which is the frequency, f, for conventional Fourier transform with a kernel of

$$K_\alpha(t_\alpha, t) = \exp(-j2\pi f t)\,. \tag{5}$$

Whereas the conventional Fourier transform is only a shift from time to frequency domain with $\alpha = 1$, the fractional

Fourier enables transformation on to any line of angle in time-frequency space, which is achieved by modifying the kernel to the form [23], [24]

$$K_\alpha(t_\alpha, t) = K_\phi \exp\left[j\pi\left(t_\alpha^2 \cot\phi - 2t_\alpha t \csc\phi + t^2 \cot\phi\right)\right] \tag{6}$$

where

$$K_\phi = |\sin\phi|^{-1/2} \exp\left[\frac{-j\pi\,\mathrm{sgn}(\sin\phi)}{4} + j\frac{\phi}{2}\right] \tag{7}$$

and

$$\phi = \frac{\alpha\pi}{2}\,. \tag{8}$$

In the case of analyzing overlapped LFM signals the transform order is optimum when it is matched to the chirp rate of the signal. To achieve maximum compression of the individual chirp components in the fractional projection, the waveform can be rotated in the fractional Fourier domain by the optimum transform order α_{opt}, which is defined as [25]

$$\alpha_{opt} = -\frac{2}{\pi}\tan^{-1}\left(\frac{1}{2a}\right)\,, \tag{9}$$

where a is the chirp rate. For a LFM signal the chirp rate is $a = B/T$ where B is the sweeping bandwidth and T is total signal duration. However, in order to calculate the optimal transform order for the discrete FrFT, the resolution of the signal both in time and frequency must be known. For the discrete case, the optimal transform order can be expressed as

$$\alpha_{opt} = -\frac{2}{\pi}\tan^{-1}\left(\frac{\Delta f/\Delta t}{2a}\right)\,, \tag{10}$$

for a system with a time resolution of Δt and frequency resolution of Δf in the interval of [-2, 2].

Since the maximum compression is achieved in the fractional Fourier domain, this can be used for analyzing the signals by recovering the time information. The projection of the time axis, μ_t, onto the fractional axis, μ_α, is calculated as

$$\mu_\alpha = \mu_t \cos(\phi)\,. \tag{11}$$

Two examples are given to show the compression capability of the FrFT. Figure 1 and Figure 2 show the fractional Fourier spectrum of two LFM chirp signals with white Gaussian noise. In both figures, each horizontal line shows the envelope of the signal at the specific fractional Fourier domain with the transform order of α, where $\alpha = 0$ is the envelope of the time domain signal and $\alpha = 1$ is the signal's frequency spectrum. The optimum transform order is calculated according to Eq.(10), which is $\alpha_{opt} = 0.5$ for this example. Note that the optimum transform angle can be between $\alpha = -2$ and $\alpha = 2$, where both angles correspond to time domain, beyond these boundaries the fractional Fourier domain is repetitive.

In Figure 1, two frequency modulated chirps are shown with a duration of 2 μs where there is a 10 μs delay between each chirp signal. This signal is transformed to the fractional Fourier domain for all α values between time domain ($\alpha = 0$) and frequency domain ($\alpha = 1$) with 0.05 increments. The maximum compression is observed at $\alpha_{opt} = 0.5$, where the chirp signal has the narrowest width in fractional time. Since both chirps have the same center frequency and bandwidth,

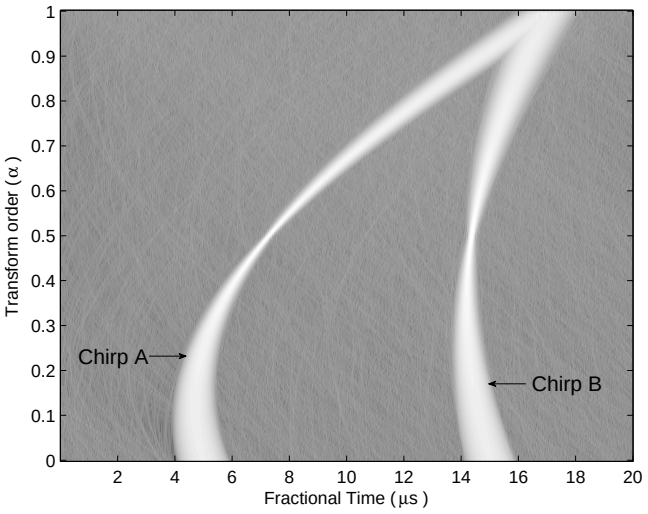

Fig. 1. Fractional Fourier transform of two different non-interfering linear frequency modulated chirps. Two chirp signals have a duration of 2 μs, center frequency of 15 MHz, bandwidth of 10 MHz and starting time of 4 μs and 14 μs.

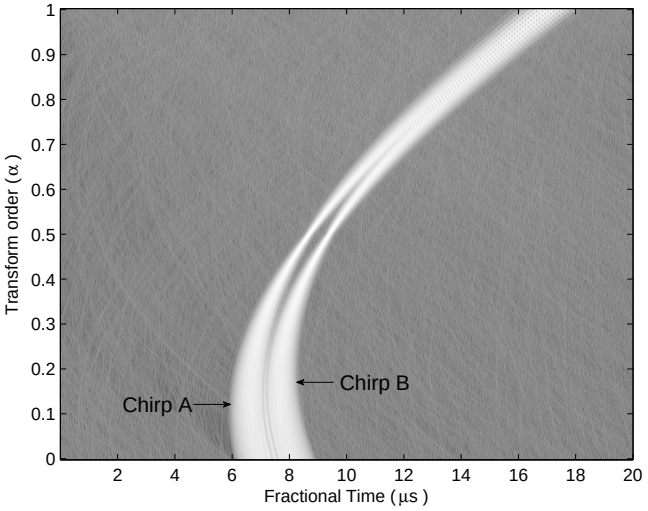

Fig. 2. Fractional Fourier transform of two interfering linear frequency modulated chirps. Two chirp signals have a duration of 2 μs, center frequency of 15 MHz, bandwidth of 10 MHz and starting time of 6 μs and 7 μs.

they overlap in the frequency domain at $\alpha = 1$. In Figure 2, two chirp signals exist with a duration of 2 μs and starting time of 6 μs and 7 μs. The interfering chirps overlap both in the time and frequency domains, where separation of the chirps is not possible in these domains. However, by using FrFT at optimum transform order ($\alpha = 0.5$), the chirp signals are maximally compressed and separation is achieved.

Rather than compression, the FrFT can also be used for filtering. Windowing in the fractional domain enables isolation of individual chirp signals [26]. After windowing, the signal can be rotated by $-\alpha_{opt}$ degrees to restore the signal to the time domain hence extracting the chirp from overlapped data. More information on fractional Fourier transform and filtering in fractional Fourier domain can be found in [23], [24], [27], [28], [29].

III. Materials and Methods

A. Experimental Setup

The experimental measurements were carried out by a 15 MHz Sonopen Replaceable Delay Line Transducer with 1 mm polystyrene tip (Olympus NDT Inc., Waltham, MA) in contact with the sample. All experiments were performed with glycerin couplant at a temperature between 21°C and 22°C. The transducer was characterized before designing the excitation waveforms and it was found that the transducer has a center frequency of 14 MHz and a -3 dB fractional bandwidth of 86%. To generate the excitation signals a 33250A Arbitrary Waveform Generator (Agilent Technologies Inc., Santa Clara, CA) was used and the signals were amplified by using E&I A150 RF Power Amplifier (Electronics & Innovation Ltd., West Henrietta, NY). Transmitted and received signals were separated by using a RDX-6 diplexer (Ritec Inc., Warwick, RI). Then the received signal was amplified by 30 dB for phantom measurements and 50 dB for tooth measurements due to the higher attenuation in enamel with a Panametrics 5072PR Pulser/Receiver (Olympus NTD Inc., Waltham, MA). All measurements were saved by a LeCroy Waverunner 64xi Oscilloscope (LeCroy Corporation, Chestnut Ridge, NY) for further processing in Matlab (Mathworks Inc., Natick, MA).

Two different measurements were performed on a tooth phantom and a human molar with the same experimental setup.

1) Phantom Measurements: The tooth phantom was constructed by bonding a 1 mm thick borosilicate glass and 1 mm thick dental composite Herculite XRV Unidose dentin (Kerr, Scafati, Italy) instead of enamel and dentin [30], where the acoustic properties of the materials are given in Table I. The thickness of the phantom layers were measured with a micrometer screw gauge (Table II). To replicate the effect of the pulp, the tooth phantom was partially immersed in water during the experiments.

2) Tooth Measurements: For the tooth measurements, an extracted human molar with intact enamel layer was burrowed from the Leeds Dental Institute Skeletal Tissues Bank. Tooth sample has been stored in a 1% aqueous thymol solution for 6 months. Before the experiments the human molar was scanned first with ultrasound and an X-ray scanner μCT 80 (Scanco Medical AG, Brüttisellen, Switzerland) with 40 μm resolution. Micro-CT data was used to validate the accuracy of the ultrasound measurements. To perform the experiments a screw thread was bonded to the tooth samples using a dental composite and cured by UV light. A high precision computer numerical controlled (CNC) positioning system with a positioning accuracy of 50 μm was used to scan the tooth sample with the ultrasound delay line transducer, as shown in Figure 3.

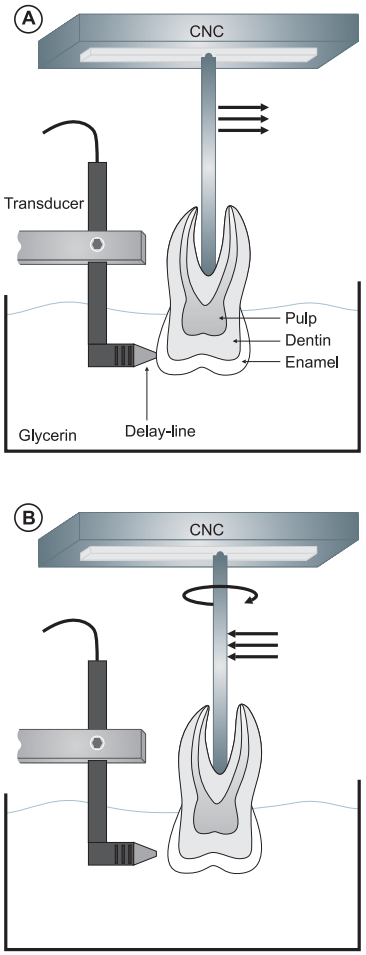

Fig. 3. Experimental setup used for enamel thickness measurements. Tooth sample is mounted to the moving arm of the CNC positioning system. Transducer is fixed by a metal profile to a stationary stage. (A) Pulse-echo measurement is done in a tank filled with glycerin. The tooth is moved away from the transducer after the measurement. (B) CNC positioning system rotates the tooth sample and moves in the opposite direction to achieve a contact with the transducer again. After the positioning the consecutive measurement is performed.

B. Coupling Material

Human tooth is a porous material. Without using any coupling material, the small air pockets between the transducer and tooth will block the ultrasonic energy transmission due to the acoustic impedance mismatch between air and enamel. In order to facilitate the transmission of ultrasound waves into the sample, a coupling material must be used. Although various acoustic couplants are evaluated for tooth imaging [31], water is usually preferred as a coupling medium for non-contact ultrasound tooth measurements [1], [3], [10], [32]. However, the acoustical mismatch between the water, polystyrene delay-line and enamel will interfere with echoes from target tissue and decrease the transmission efficiency. In this study, glycerin is chosen as the coupling material to fill the small pores on the tooth surface. Since glycerin and polystyrene nearly have same acoustic impedances (Table I), the transfer efficiency is improved by minimizing the impedance mismatch.

C. Contact Imaging

For the measurements, tooth sample and the transducer were immersed in a tank filled with glycerin and controlled by a CNC positioning system. Even there was a glycerin couplant between the delay-line and tooth sample, the measurements were performed in contact mode, where the glycerin was only used to fill the microscopic pores on the surface of the tooth sample.

TABLE II
THICKNESS MEASUREMENTS

	Glass	Dental composite	A.E.	M.A.E.
Actual Size	0.998 mm	1.016 mm		
Gaussian Pulse	1.006 mm	0.951 mm	36 μm	65 μm
MF (Short LFM)	1.039 mm	1.050 mm	37 μm	41 μm
FrFT (Short LFM)	1.048 mm	1.060 mm	46 μm	50 μm
MF (Long LFM)	1.030 mm	0.975 mm	36 μm	41 μm
FrFT (Long LFM)	0.970 mm	1.012 mm	16 μm	28 μm

* (A.E.) Average error, (M.A.E.) Maximum absolute error

For the proposed contact imaging technique, transducer positioning and having a good contact with the tooth sample is crucial for accurate measurements. The human tooth however has a rough and curved surface, which makes it difficult to achieve a good contact with the probe tip. This contact problem between the tooth and transducer was solved by checking the phase of first reflected echo. In the experiments, the acoustic impedances of the polystyrene, glycerin and enamel was used to verify contact between the delay-line and enamel by considering the 180° phase shift of the returned echo while the transducer is coupling to the enamel. Measurements were also performed on the tooth phantom to test the proposed contact verification method, where results are given in Experiments section.

A similar contact problem was reported by Louwerse *et al.* [16] to show the error in enamel thickness measurements due to variations in positioning of the probe tip. In this work, the contact problem was solved by checking the phase of the reflected signal and by using a CNC positioning system to increase the reproducibility of the measurements. The importance of reproducibility of ultrasonic enamel thickness measurements and the variations is further discussed by Louwerse [16].

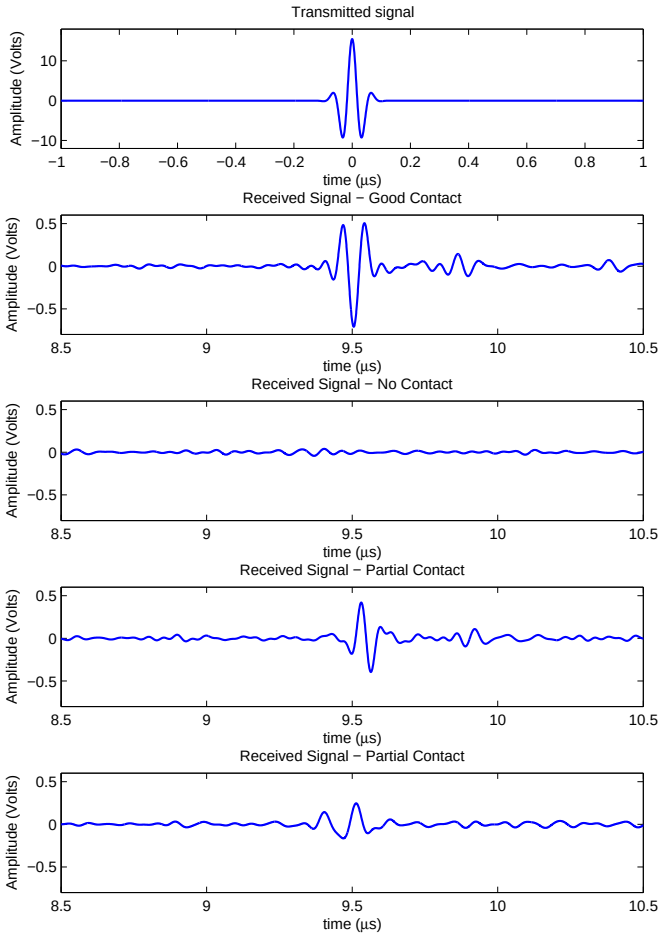

Fig. 4. (First) Transmitted Gaussian pulse. (Second) Received signal from a good contact, where a phase-shifted Gaussian pulse can be seen at 9.5 μs. (Third) Received signal without any contact, where no reflections can be observed. (Fourth) Received signal from a partial contact, where the observed phase shift is not 180°. (Fifth) Received signal from a partial contact, where the shape of the Gaussian pulse is distorted.

IV. EXPERIMENTS

To verify the accuracy of the proposed coded excitation scheme and the fractional Fourier technique, first measurements were performed on a tooth phantom of known dimensions. The excitation method was also compared with a Gaussian pulse of the same bandwidth, which is widely used by researchers to measure the thickness of the tooth layers [2], [10], [3], [11], [33], [32], [34].

A. Contact Verification

In all experiments, the phase of the first reflected echo was used to verify contact between the transducer delay-line and tooth sample or tooth phantom. However, before performing the thickness measurements, the contact verification method was tested on the tooth phantom. Transmitted signal was captured as shown in Figure 4 (first) and this measurement was used as a control signal, where a 180° phase shift must be observed when the contact between the delay-line and enamel is achieved. This phase shift appears, because the imaging system has two physical interfaces; 1) between the transducer and the delay-line, 2) between the delay-line and tooth. The polystyrene delay-line has a lower acoustic impedance than the transducer (PZT-5A) resulting in a negative reflection coefficient,

$$\Gamma = \frac{\mathrm{Z}_{polystyrene} - \mathrm{Z}_{transducer}}{\mathrm{Z}_{polystyrene} + \mathrm{Z}_{transducer}} < 0\,. \tag{12}$$

However while coupling from the polystyrene delay-line to enamel, the reflection coefficient is positive;

$$\Gamma = \frac{\mathrm{Z}_{enamel} - \mathrm{Z}_{polystyrene}}{\mathrm{Z}_{enamel} + \mathrm{Z}_{polystyrene}} > 0\,. \tag{13}$$

Since two reflection coefficients has different signs, a 180° phase shift is expected between the signal at $t = 0$ and $t = 9.5$ μs in Figure 4. For a good contact, 180° phase shift was observed between Figure 4 (first) and Figure 4 (second), which was considered as valid measurement. However if the waveform is distorted or the phase shift is not 180°, the ultrasound measurement was discarded. Figure 4 (third), Figure 4 (fourth) and Figure 4 (fifth) are some examples, where the measurements were discarded due to the aforementioned phase shift technique could not be verified.

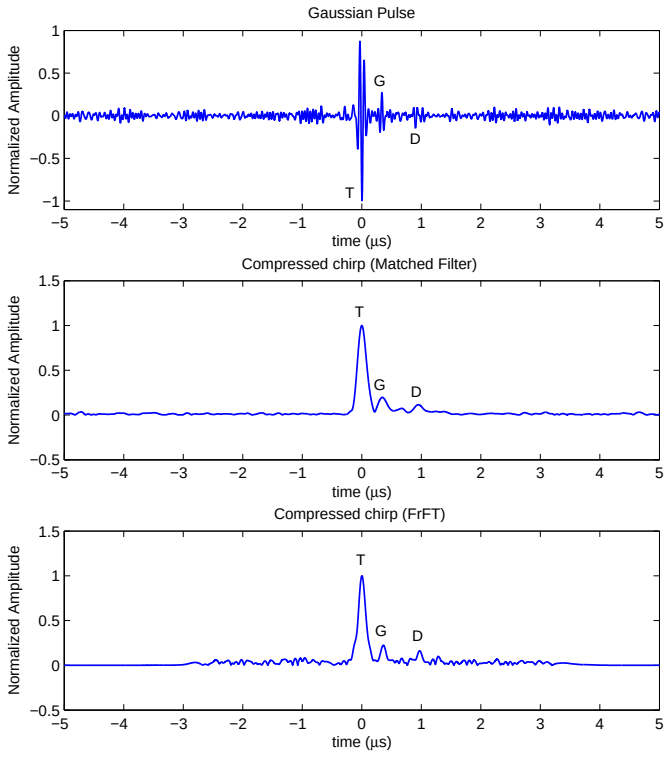

Fig. 5. Comparison of Gaussian pulse with LFM chirp after compressing with matched filter and FrFT. (T) denotes the reflection from transducer tip and glass boundary. (G) denotes the reflection from glass and dental composite boundary. (D) denotes the reflection from dental composite and water boundary.

B. Thickness Measurements on Tooth Phantom

The tooth phantom was measured with three different excitation signals; a Gaussian pulse, a short LFM signal with 0.5 μs duration, and a long LFM signal with 2 μs duration. All signals were designed to match the transducer frequency response, and therefore a center frequency of 14 MHz and a fractional bandwidth of 80% were chosen. A Hann window was applied to the LFM signals to reduce the side lobe levels after compression. The same excitation voltage of 25 V_{pp} was used in each measurement.

The Gaussian pulse was chosen to demonstrate the basic pulse-echo technique and the measurements performed with the Gaussian pulse were filtered using a band-pass filter. However, to compress the interfered chirp signals, the LFM measurements were first filtered using a band-pass filter and then processed using the FrFT technique or matched filter. Two different MFs were designed for short and long duration LFM signals by using the time-reversed complex conjugate of the transmitted chirps [19]. These were then used to compress the received signals. FrFT was performed at $\alpha = 1.7421$ for the short LFM and at $\alpha = 1.3360$ for the long LFM, where the rotation angle is calculated according to Equation (10). In phantom thickness measurements, both techniques were only used for compression.

The received echoes for the Gaussian pulse and the envelope of received signal for the LFM excitation after compressing with MF and FrFT are shown in Figure 5, respectively. The time-of-flight between consecutive pulses or compressed chirps, which are denoted as **T**, **G** and **D** in the Figure 5, were measured. The time-of-flight information for the signals in the fractional Fourier domain was recovered by using Eq. (11). The layer thicknesses were calculated through prior knowledge of the speed of sound in that material, which is given in Table I. The average error and maximum absolute error for each method was calculated and the accuracy of the techniques is compared using the results given in Table II. Of the tested techniques, it is found that the LFM signal with 2 μs duration processed with the FrFT technique gives the minimal error, which is less than the half of a Gaussian pulse.

C. Enamel Thickness Measurement

To measure the enamel thickness of the human molar, the tooth sample was mounted to the moving arm of the CNC positioning system. The transducer was fixed on a stationary stage and pulse-echo measurements performed with chirp excitation. Measurement data was obtained through automated CNC scanning performed in steps of 5°, as shown in Figure 3. Only the LFM signal was used for excitation with a duration of 2 μs, center frequency of 14 MHz, fractional bandwidth of 80%, and excitation voltage of 25 V_{pp}, which approximately generates a pressure of 150 kPa inside the enamel.

The ultrasound data was processed in two different ways. In Figure 6 (top), the matched filter technique was used to compress the received ultrasound echoes. In Figure 6 (bottom), the received signals were transformed to the fractional Fourier domain where the rotation angle was calculated by Equation (10). The temporal information was recovered back by scaling the time axis according to Equation (11). By comparing these figures, it can be observed that the FrFT technique gives a better compression with a smaller main lobe width and hence better resolution in the final image, where the features of the tooth are more distinguishable such as the DEJ at the north-east of Figure 6 (bottom).

For the tooth measurements, the received signal is attenuated not only because of depth and frequency dependant attenuation, but also because of scattering, dispersion and absorption [2]. The structure of the dental tissues absorbs and scatters the sound wave unexpectedly due to roughness and the irregular curved shape of the tooth. The overall effect on the received echo is degraded SNR, change in the envelope shape and reduced bandwidth, which will result in a discrepancy between the MF and chirp signal. This phenomenon was observed in the real tooth measurements. Figure 7 shows the worst case observed in the measurements, where it was not possible to measure the enamel thickness correctly with the compression achieved by the matched filter. In Figure 7 (middle) the reflected echoes from enamel surface, enamel-dentin boundary and second reflection from enamel-dentin boundary appears as a single lobe after compression. In this case, the search algorithm, which uses the *findpeaks* function in Matlab to find the local maxima, located the false DEJ according to the second reflection from enamel-dentin boundary. However, in Figure 7 (bottom) the compression achieved by the FrFT clearly shows the difference between

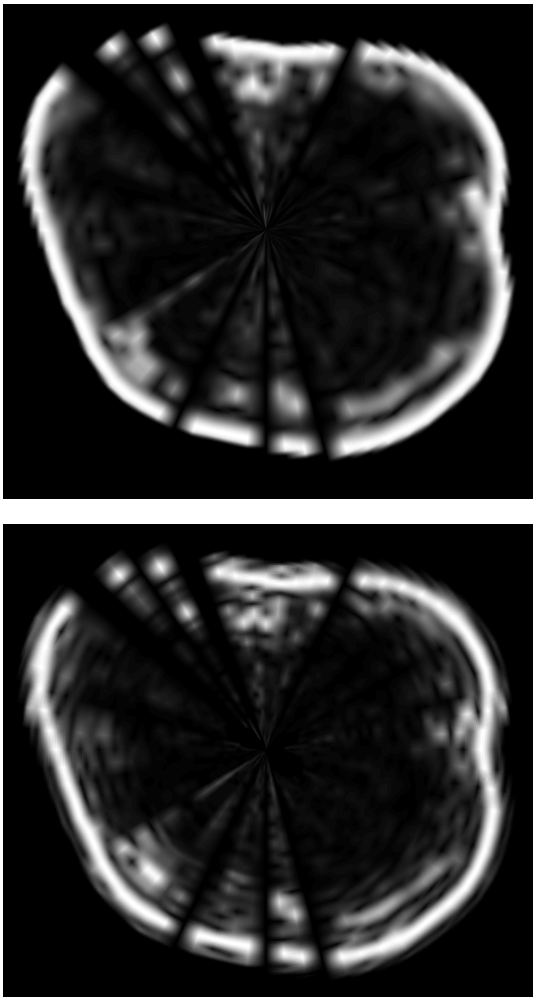

Fig. 6. Ultrasound image of the tooth scanned with a LFM signal and processed with MF technique (top) and FrFT technique (bottom). This scan is performed to measure the enamel thickness of the tooth.

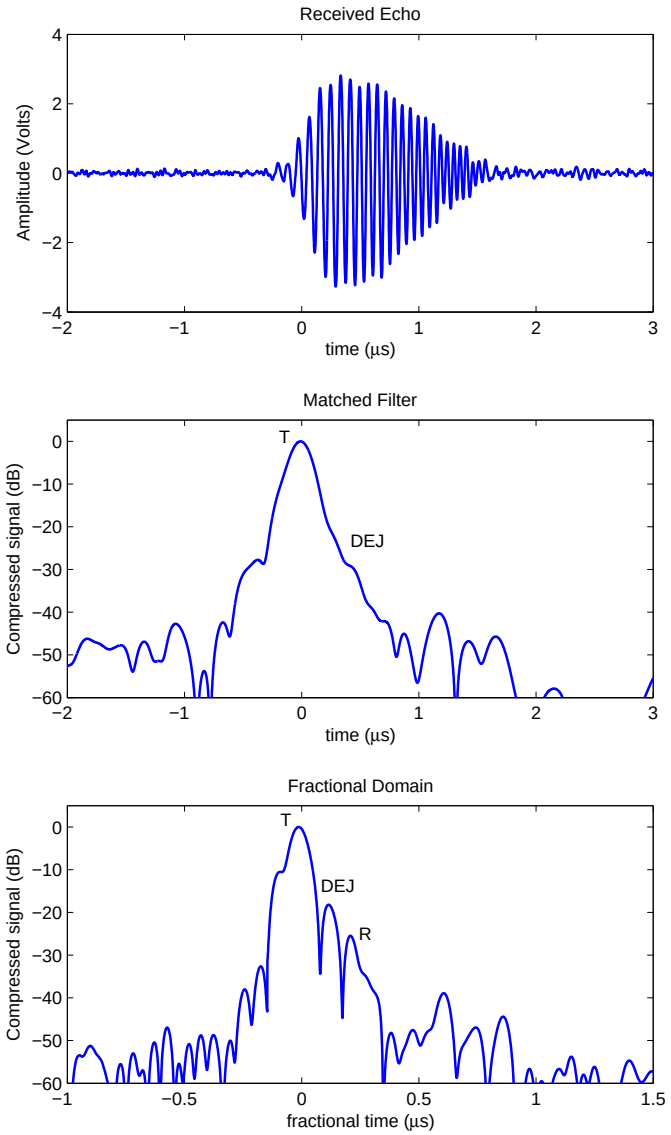

Fig. 7. Received signal (top), compressed signal with matched filter (middle) and signal transformed to fractional Fourier domain to achieve compression (bottom). (T) denotes the reflection from transducer tip and enamel boundary. (DEJ) denotes the reflection from dentino-enamel junction. (R) denotes the reverberation (secondary internal reflection) caused by the enamel-dentin boundary.

each reflection. In this example, the advantage of the FrFT over the MF becomes more obvious; transforming the signals into fractional Fourier domain gives the best compression and hence increases the probability of the detection of echoes.

In order to compare the accuracy of the FrFT and MF, the enamel thickness measurements processed with both techniques were plotted on the X-ray scan of the tooth, as shown in Figure 8. The registration of the Micro-CT slice with the ultrasound data was done by using the positional information of the transducer relative to the tooth sample, which was controlled by the CNC system. In the Table I the typical acoustic properties of the materials used are shown. Thickness of the tooth layers were calculated according to these values by using the time-of-flight measurements.

In the Figure 8, some measurement points between 115° and 145° are missing, because good contact between the enamel and the transducer tip cannot be achieved due to the curvature of the tooth surface. A similar problem was also observed for the measurement points of 70°, 235°, 275°, and 290°. The measurement data for these angles were discarded after checking the phase of the reflection from enamel surface. The compression problem explained in Figure 7 was observed at 10°, 30°, 125°, 160°, 190°, 210° and 340°, which increases the error for the MF technique.

In order to compare the real values with the data processed by the FrFT and MF techniques, an edge detection algorithm was used to measure actual enamel thickness from the Micro-CT image. The edge detection was performed by the *edge* function based on the Sobel method in Matlab, which finds edges in the image using the Sobel approximation to the derivative of the Micro-CT data. The maximum relative error observed for the MF was 113% and the maximum absolute error was 860 μm, which was expected because of the aforementioned compression problem. However the maximum relative error for the FrFT was 33% and the maximum absolute error was 370 μm. The average relative error values are also calculated in order to make a fair comparison between the

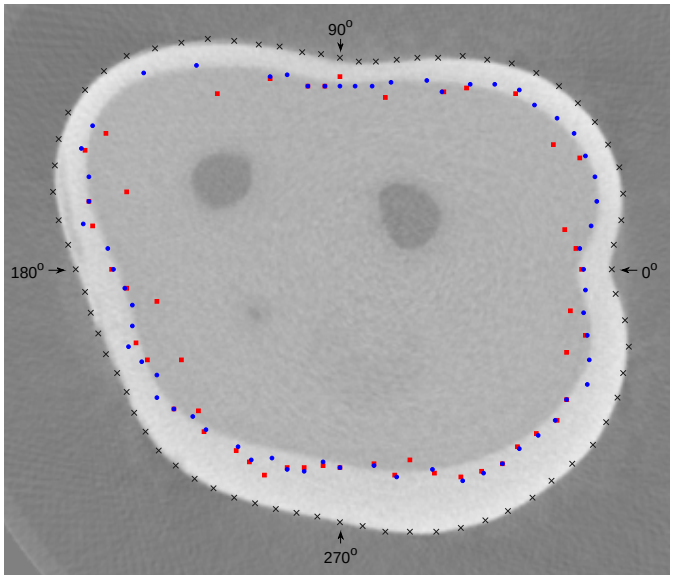

Fig. 8. Figure shows the ultrasound enamel thickness measurements mapped on Micro-CT image. Black crosses represent the outer surface of the tooth. Blue dots show the ultrasound measurements processed with FrFT. Red squares show the ultrasound measurements processed with matched filter. The image dimensions are 14 mm × 12 mm.

phantom and tooth measurements. The mean absolute error for the FrFT was 45 μm and the average relative error was calculated as 5.5%, which was higher than the 1.6% error achieved in the phantom measurements for the same technique. The mean absolute error calculated for the MF was 109 μm and the average relative error was 13.4%, which was more than double of the error observed for the FrFT.

V. Discussion

In this work, time-of-flight measurement for a human molar was performed with a delay-line transducer in contact mode. The use of similar transducers, such as delay-line or thickness gauge, is common for dental measurements [16], [35], [36]. Researchers, who used similar transducers, concluded that ultrasonic measurement of enamel thickness is feasible without any enamel preparation. This improves the *in-vivo* applicability of the proposed contact imaging technique, since teeth can be examined without cleaning or any further processing. However, SAM can achieve better resolution and perform more accurate measurements [9], [37], but it cannot be used practically for real-time *in-vivo* diagnostic imaging in dentistry.

The main limitation of this method, time-of-flight measurement, is that the velocity of the medium must be known *a priori*. However, without knowing the exact speed of sound in tooth layers, the average velocity values can be used with a cost of increased error. In this study, experiments are performed on two different samples; a phantom with known material properties and a human tooth. Tooth phantom measurements showed that the thickness of the glass and dental composite can be measured with a 1.6% error, where the average error increased to 5.5% for the real tooth sample using the FrFT technique. The average error for the matched filter was calculated as 3.6% for the tooth phantom and 13.4% for the real tooth measurements. The error for the FrFT technique is within the speed of sound variations observed for different tooth samples. The average speed of sound measured by several researchers is 6250 m/s with a deviation of $\pm$ 410 m/s [2]. In a study focused on enamel thickness measurements, researchers used an average speed of sound of 6500 m/s and reported an average error of 50 μm [35]. This is similar with mean absolute error of 45 μm for the FrFT technique observed in this study, which is based on using averaged speed of sound values.

For the experiments performed with human teeth, it is difficult to evaluate the accuracy of the measurement technique since this study was based on the average sound velocities in dental tissues. The speed of sound varies in different sections of enamel and dentin layers even within the same sample [38]. It was previously reported that there is a great variance between measured tooth samples [2], [3]. Additionally, ultrasonic wave propagation in human teeth is not trivial due to the anisotropic structure of tooth, where the speed of sound can vary within the same tooth in different directions [39], [38]. In Figure 8, for angles between 300° and 325° the ultrasound measurements did not match with the X-ray scan of the tooth. The reason for the mismatch is the anisotropic structure of the tooth. It was measured that the density of the enamel layer between these angles was roughly 9% higher than the average enamel density. Rose *et al.* showed the correlation between the sound velocity and bone mineral density in tooth [40], where higher mineral density increases the speed of sound. This is the reason why the enamel thickness measured less in this region.

For *in-vivo* tooth measurements, the expected error will be similar with the *ex-vivo* measurements performed in this study. It is shown that by storing the tooth sample in aqueous solutions, the mechanical properties of tooth can be protected [9]. The speed of sound will be similar for a moist extracted tooth and non-extracted tooth, where the hardness and the sound velocity of the tooth will crucially change after drying [41]. In this study, the tooth sample was always stored in an aqueous solution in order to eliminate the drying effect. Temperature will be another important variable for the *in-vivo* and *ex-vivo* measurements. However, it is proven that the measurements performed at 21°C and 34°C do not have significant difference for a human incisor teeth [35].

VI. Conclusions

In optics and signal processing the fractional Fourier transform (FrFT) has many applications, although there are only a few examples of the application of FrFT in ultrasound [42], [43], [26]. In this study, the ultrasonic non-destructive evaluation of human teeth using chirp coded excitation together with FrFT was performed. The FrFT was used for the first time to analyze the received echoes by separating chirp signals overlapping in both the time and frequency domains in dental imaging. The proposed technique was used to measure the thickness of the enamel layer in human tooth.

Besides measuring the thickness of tooth layers, other possible applications for this method are locating the cracks

inside the tooth and analyzing the restoration faults under the fillings. Dentists appeal to visual and endodontic examination methods or dental radiographs to diagnose cracked teeth. These methods are usually not effective in the early detection of cracks before the crack causes an infection [5]; however the coded excitation improves the detectability of the small cracks by increasing the SNR. Another major problems encountered in dentistry is the bonding faults between dental composite and tooth. Conventional radiography cannot be used for imaging of radiopaque restoration material, but the ultrasound is able to penetrate into the hard structures and can detect cavities under existing restorations [11], [44]. The proposed contact imaging method combined with coded excitation and the FrFT technique can be used as a diagnostic tool in dentistry to measure the enamel thickness, locate the cracks inside the tooth and analyze the possible restoration faults.

ACKNOWLEDGMENT

The authors would like to thank Professor Richard M. Hall, Khalid Sindi, and Ondrej Holub of University of Leeds for their valuable support during this work.

The use of human teeth for this study was approved by the Leeds Dental Institute Skeletal Tissues Bank which is in turn approved by the National Health Service Research Ethics Committee (UK) (ref: 07H130693), according to the Human Tissues Act 2004 (UK).

REFERENCES

[1] G. Kossoff and C. Sharpe, "Examination of the contents of the pulp cavity in teeth," *Ultrasonics*, vol. 4, no. 2, pp. 77–83, 1966.

[2] F. Barber, S. Lees, and R. Lobene, "Ultrasonic pulse-echo measurements in teeth," *Archives of Oral Biology*, vol. 14, no. 7, pp. 745–760, 1969.

[3] S. Ghorayeb and T. Valle, "Experimental evaluation of human teeth using noninvasive ultrasound: echodentography," *Ultrasonics, Ferroelectrics and Frequency Control, IEEE Transactions on*, vol. 49, no. 10, pp. 1437–1443, 2002.

[4] J. Hua, S.-K. Chen, and Y. Kim, "Refining enamel thickness measurements from b-mode ultrasound images," in *Proceedings of IEEE Engineering in Medicine and Biology Society*, 2009, pp. 440–443.

[5] M. Culjat, R. Singh, E. Brown, R. Neurgaonkar, D. Yoon, and S. White, "Ultrasound crack detection in a simulated human tooth," *Dentomaxillofac Radiology*, vol. 34, no. 2, pp. 80–85, 2005.

[6] D. Hughes, J. Girkin, S. Poland, C. Longbottom, T. Button, J. Elgoyhen, H. Hughes, C. Meggs, and S. Cochran, "Investigation of dental samples using a 35 mhz focussed ultrasound piezocomposite transducer," *Ultrasonics*, vol. 49, no. 2, pp. 212–218, 2008.

[7] R. G. Maev, L. A. Denisova, E. Y. Maeva, and A. A. Denissov, "New data on histology and physico-mechanical properties of human tooth tissue obtained with acoustic microscopy," *Ultrasound in Medicine & Biology*, vol. 28, no. 1, pp. 131–136, 2002.

[8] S. Peck and G. Briggs, "The caries lesion under the scanning acoustic microscope," *Advances in Dental Research*, vol. 1, no. 1, pp. 50–63, 1987.

[9] K. Raum, K. Kempf, H. J. Hein, J. Schubert, and P. Maurer, "Preservation of microelastic properties of dentin and tooth enamel in vitroa scanning acoustic microscopy study," *Dental Materials*, vol. 23, no. 10, pp. 1221–1228, 2007.

[10] C. Löst, K.-M. Irion, C. John, and W. Nüssle, "Two-dimensional distribution of sound velocity in ground sections of dentin," *Dental Traumatology*, vol. 8, no. 5, pp. 215–218, 1992.

[11] M. Culjat, R. Singh, D. Yoon, and E. Brown, "Imaging of human tooth enamel using ultrasound," *Medical Imaging, IEEE Transactions on*, vol. 22, no. 4, pp. 526–529, 2003.

[12] R. Singh, M. Culjat, R. Neurgaonkar, S. White, W. Grundfest, and E. Brown, "Single-element plzt transducer for wide-bandwidth imaging of solid materials," in *IEEE Ultrasonics Symposium*, 2006, pp. 1926–1930.

[13] S. Ghorayeb, C. Bertoncini, and M. Hinders, "Ultrasonography in dentistry," *Ultrasonics, Ferroelectrics and Frequency Control, IEEE Transactions on*, vol. 55, no. 6, pp. 1256–1266, 2008.

[14] B. Rosenberg, P. E. Murray, and K. Namerow, "The effect of calcium hydroxide root filling on dentin fracture strength," *Dental Traumatology*, vol. 23, no. 1, pp. 26–29, 2007.

[15] C. R. Dugmore and W. P. Rock, "A multifactorial analysis of factors associated with dental erosion," *British Dental Journal*, vol. 196, no. 5, pp. 283–286, 2004.

[16] C. Louwerse, M. Kjaeldgaard, and M. C. D. N. J. M. Huysmans, "The reproducibility of ultrasonic enamel thickness measurements: an in vitro study," *Journal of Dentistry*, vol. 32, no. 1, pp. 83–89, 2004.

[17] G. S. Kino, *Acoustic Waves:Devices, Imaging, and Analog Signal Processing*, R. Woods, Ed. Prentice-Hall, Inc., 1987.

[18] M. I. Skolnik, *Introduction to Radar Systems*, F. J. Cerra, Ed. McGraw-Hill, 1981.

[19] T. Misaridis and J. Jensen, "Use of modulated excitation signals in medical ultrasound. part i: basic concepts and expected benefits," *Ultrasonics, Ferroelectrics and Frequency Control, IEEE Transactions on*, vol. 52, no. 2, pp. 177–191, 2005.

[20] R. Chiao and X. Hao, "Coded excitation for diagnostic ultrasound: a system developer's perspective," *Ultrasonics, Ferroelectrics and Frequency Control, IEEE Transactions on*, vol. 52, no. 2, pp. 160–170, 2005.

[21] V. Namias, "The fractional order Fourier transform and its application to quantum mechanics," *IMA Journal of Applied Mathematics*, vol. 25, no. 3, pp. 241–265, 1980.

[22] A. C. McBride and F. H. Kerr, "On Namias's fractional Fourier transforms," *IMA Journal of Applied Mathematics*, vol. 39, no. 2, pp. 159–175, 1987.

[23] H. Ozaktas, O. Arıkan, M. Kutay, and G. Bozdağı, "Digital computation of the fractional Fourier transform," *Signal Processing, IEEE Transactions on*, vol. 44, no. 9, pp. 2141–2150, 1996.

[24] Ç. Candan, M. Kutay, and H. Ozaktas, "The discrete fractional Fourier transform," *Signal Processing, IEEE Transactions on*, vol. 48, no. 5, pp. 1329–1337, 2000.

[25] C. Capus and K. Brown, "Short-time fractional Fourier methods for the time-frequency representation of chirp signals," *Journal of the Acoustical Society of America*, vol. 113, no. 6, pp. 3253–3263, 2003.

[26] D. Cowell and S. Freear, "Separation of overlapping linear frequency modulated (LFM) signals using the fractional Fourier transform," *Ultrasonics, Ferroelectrics and Frequency Control, IEEE Transactions on*, vol. 57, no. 10, pp. 2324–2333, 2010.

[27] L. Almeida, "The fractional Fourier transform and time-frequency representations," *Signal Processing, IEEE Transactions on*, vol. 42, no. 11, pp. 3084–3091, 1994.

[28] H. Ozaktas, B. Barshan, D. Mendlovic, and L. Onural, "Convolution, filtering, and multiplexing in fractional Fourier domains and their relation to chirp and wavelet transforms," *Journal of the Optical Society of America A*, vol. 11, no. 2, pp. 547–559, 1994.

[29] A. Kutay, H. Ozaktas, O. Arıkan, and L. Onural, "Optimal filtering in fractional Fourier domains," *Signal Processing, IEEE Transactions on*, vol. 45, no. 5, pp. 1129–1143, 1997.

[30] R. S. Singh, M. O. Culjat, W. S. Grundfest, E. R. Brown, and S. N. White, "Tissue mimicking materials for dental ultrasound," *The Journal of the Acoustical Society of America*, vol. 123, no. 4, pp. EL39–EL44, 2008.

[31] M. O. Culjat, R. S. Singh, S. N. White, R. R. Neurgaonkar, and E. R. Brown, "Evaluation of gallium-indium alloy as an acoustic couplant for high-impedance, high-frequency applications," *Acoustics Research Letters Online*, vol. 6, no. 3, pp. 125–130, 2005.

[32] C. John, "Directing ultrasound at the cemento-enamel junction (cej) of human teeth: I. asymmetry of ultrasonic path lengths," *Ultrasonics*, vol. 43, no. 6, pp. 467–479, 2005.

[33] S. Ghorayeb, T. Xue, and W. Lord, "Ultrasonic imaging of teeth for early detection of abscesses," in *IEEE Ultrasonics Symposium, 1997.*, 1997, pp. 1511–1515.

[34] C. John, "Lateral distribution of ultrasound velocity in horizontal layers of human teeth," *The Journal of the Acoustical Society of America*, vol. 119, no. 2, pp. 1214–1226, 2006.

[35] M. C. D. N. J. M. Huysmans and J. M. Thijssen, "Ultrasonic measurement of enamel thickness: a tool for monitoring dental erosion?" *Journal of Dentistry*, vol. 28, no. 3, pp. 187–191, 2000.

[36] F. Yanıkoğlu, F. Öztürk, O. Hayran, M. Analoui, and G. Stookey, "Detection of natural white spot caries lesions by an ultrasonic system," *Caries Research*, vol. 34, pp. 225–232, 2000.

[37] O. Marangos, A. Misra, P. Spencer, and J. L. Katz, "Scanning acoustic microscopy investigation of frequency-dependent reflectance of acid-etched human dentin using homotopic measurement," *Ultrasonics, Ferroelectrics and Frequency Control, IEEE Transactions on*, vol. 58, no. 3, pp. 585–595, 2011.
[38] S. Ghorayeb, P. Petrakis, and M. McGrath, "Experimental determination of ultrasonic phase velocities in human teeth along arbitrary symmetry directions," in *Proceedings of IEEE Engineering in Medicine and Biology Society, 2003.*, vol. 3, 2003, pp. 2382–2385.
[39] S. Lees and F. R. Jr., "Anisotropy in hard dental tissues," *Journal of Biomechanics*, vol. 5, no. 6, pp. 557–566, 1972.
[40] E. Rose, M. Hagenmüller, I. Jonas, and B. Rahn, "Validation of speed of sound for the assessment of cortical bone maturity," *European Journal of Orthodontics*, vol. 27, no. 2, pp. 190–195, 2005.
[41] V. P. Totah, "Increase in hardness of dentin on drying," *Journal of Dental Research*, vol. 21, pp. 99–101, 1942.
[42] M. Bennett, S. McLauglin, T. Anderson, and N. McDicken, "Filtering of chirped ultrasound echo signals with the fractional Fourier transform," in *IEEE Ultrasonics Symposium*, vol. 3, 2004, pp. 2036–2040.
[43] S. Harput, D. M. J. Cowell, J. A. Evans, N. Bubb, and S. Freear, "Tooth characterization using ultrasound with fractional Fourier transform," in *IEEE Ultrasonics Symposium*, 2009, pp. 1906–1909.
[44] R. Singh, M. Culjat, J. Cho, R. Neurgaonkar, D. Yoon, W. Grundfest, E. Brown, and S. White, "Penetration of radiopaque dental restorative materials using a novel ultrasound imaging system," *American Journal of Dentistry*, vol. 20, no. 4, pp. 221–226, 2007.

Sevan Harput received the B.Sc. degree in microelectronics engineering and the M.Sc. in electronic engineering and computer sciences from Sabancı University, Turkey in 2005 and 2007, respectively. He worked as a teaching and research fellow in Sabancı University between 2007 and 2008. In 2009, he joined to the Ultrasound Group in the School of Electronic and Electrical Engineering, University of Leeds. He is working as a research and teaching assistant in the University of Leeds. His research interests include ultrasound medical imaging, nonlinear acoustics and ultrasound contrast agents.

Dr. Tony Evans gained his Ph.D. in Electronic Engineering 1986 from the University of Wales. He was appointed Lecturer and then Senior Lecturer at the University of Leeds in 1986 and 2002 respectively. He is a Past-President of the British Medical Ultrasound Society. Current areas of research include an evaluation of the image quality of ultrasound systems used for screening for breast cancer, fetal anomalies and aortic aneurysms and he is a co-investigator in the Engineering and Physical Sciences Research Council funded project Engineering Therapeutic Microbubbles. He is the course director for the M.Sc. in Medical Physics.

Dr. Nigel Bubb gained his first degree as a materials scientist in '92 having previously worked as a dental technician. Since then he has worked in the field of dental materials, latterly at Leeds Dental Institute at the University of Leeds, where in 2002 he gained his PhD in glass ceramics. His current role as Fellow in Dental Materials has both teaching and research threads. Teaching: dental materials in a number of programmes and managing several modules. Research: glass ceramics, air abrasion of teeth and imaging of dental materials using ultrasound.

Dr. Steven Freear gained his doctorate in 1997 and subsequently worked in the medical electronics industry for 7 years. He was appointed Lecturer and then Senior Lecturer in 2006 and 2008 respectively at the School of Electronic and Electrical Engineering at the University of Leeds. In 2006 he formed the Ultrasound Group specializing in both industrial and biomedical research. Current projects include and Engineering and Physical Sciences Research Council funded project Engineering Therapeutic Microbubbles and acoustic instrumentation for BP. His main research interest is concerned with advanced analogue and digital signal processing and instrumentation. He teaches digital signal processing, microcontrollers/microprocessors, VLSI and embedded systems design, hardware description languages at both undergraduate and postgraduate level.